

# Effect of cooling rates from partial solution temperature and aging on $\gamma'$ precipitation in IN792 superalloy

H. Arabi<sup>1</sup>, S. Rastegari<sup>2</sup>, M. Mirhosseini<sup>3</sup> and B. M. Sadeghi\*<sup>2</sup>

One of the important factors affecting the microstructure of Ni base superalloys is the cooling rate from partial solution temperature; therefore, the prime purpose of the present research is to investigate the effects of this factor on some microstructural features of superalloy IN792. The results showed that by increasing the cooling rate from 5 to 160°C min<sup>-1</sup> after partial solution treatment at 1120°C for 2 h, the size and volume fraction of primary  $\gamma'$  decreased, but during the subsequent aging the volume fraction of secondary  $\gamma'$  increased initially exponentially and later linearly. When high cooling rates >90°C min<sup>-1</sup> were applied, the formation of secondary  $\gamma'$  was totally suppressed. However, after aging at 845°C for a period of 24 h, the amount of secondary  $\gamma'$  increased with a decelerating rate up to 60°C min<sup>-1</sup> and then with a linear rate up to 160°C min<sup>-1</sup>. The later observation has not been reported elsewhere.

**Keywords:** IN792, Superalloy, Cooling rate,  $\gamma'$  phase, Heat treatment

## Introduction

Ni base superalloys are very suitable materials for high temperature applications due to their ability to keep their high strength at a temperature as high as 80% of their melting point. Considering the complexity of nickel based superalloy microstructures, it is essential to control the effective processing parameters on the microstructures of these types of alloys in order to prevent the formation of harmful phases and be able to develop useful features for specific application. The microstructure of this type of alloy in general includes a solid solution matrix of nickel known as  $\gamma$  with FCC structure, primary and secondary  $\gamma'$  phases with Ni<sub>3</sub> (Al, Ti) composition having L1<sub>2</sub> structure; eutectic of  $\gamma'/\eta$ ; and some strengthening carbides such as MC, M<sub>6</sub>C and M<sub>23</sub>C<sub>6</sub>.<sup>1</sup> Other harmful needle shape or Chinese script shape phases such as laves and  $\sigma$  might be present in their microstructure if processing is not controlled carefully.<sup>2</sup>

The high strength of these alloys is basically due to the strength of solid solution  $\gamma$  matrix and coherent  $\gamma'$  particles that usually appear in the form of large cubic primary  $\gamma'$  and small spherical secondary  $\gamma'$ .<sup>2</sup> The characteristics of the  $\gamma'$  phase can directly affect the mechanical properties of these alloys.<sup>1-4</sup> These characteristics are a function of the composition and type of

processing parameters, such as heat treatment applied on these types of alloys.<sup>1-6</sup> The principle objective of full solution treatment is to put hardening phases into solution and dissolve some carbide. However, since the utilisation of higher solution treating temperature for a long time will result in some grain growth, more extensive dissolving of carbides, melting of eutectic phase particularly in the vicinity of grain boundaries, and possible formation of continuous MC carbides within grain boundaries, it would be better to perform this operation in two steps. One should bear in mind that when more than one phase is capable of precipitating from the alloy matrix during heat treatment a judicious selection of assign solution and aging treatments that produce different sizes and types and better distribution of precipitates at different temperature is very important. Therefore, in the present research, in addition to the application of a full solution for a short time to homogenise the microstructure, partial solution at lower temperature was also used to stabilise the microstructure and form discontinuous carbides at grain boundaries.

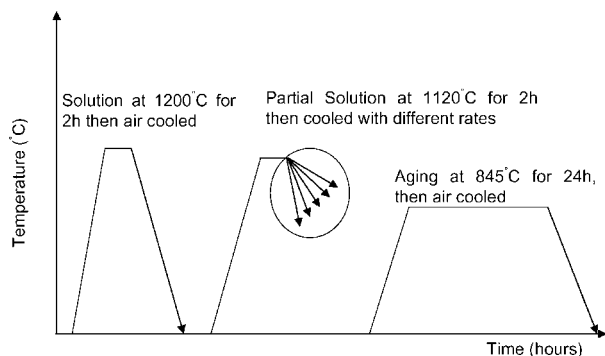
Some researches<sup>7-9</sup> have pointed out the importance of cooling rate from partial solution temperature on the microstructure of some Ni base superalloys. For example, Koul *et al.*<sup>7</sup> reported by increasing the cooling rate from partial solution temperature the size of  $\gamma'$  decreases, while other researchers<sup>8</sup> on Udimet 720Li showed that the sizes of  $\gamma'$  precipitates are insensitive to the cooling rate after solution treatment. It has also been reported<sup>9</sup> that the presence of elements Re and W in the superalloy CMSX-4 reduces the sensitivity of  $\gamma'$  growth to cooling rate because of the delay that occurs in the diffusion process. In addition to the size of  $\gamma'$ , a severe

<sup>1</sup>Center of Excellence for High Strength Alloys Technology (CEHSAT), School of Metallurgy and Materials Engineering, Iran University of Science and Technology (IUST), Narmak, Tehran, Iran

<sup>2</sup>School of Metallurgy and Materials Engineering, IUST, Narmak, Tehran, Iran

<sup>3</sup>IUST, Narmak, Tehran, Iran

\*Corresponding author, email bmsadeghi@yahoo.com



1 Schematic of heat treatment cycles

reduction in volume fraction of  $\gamma'$  precipitates with increasing cooling rate has been reported by Sajjadi *et al.*<sup>10</sup> for Ud500 and Mao *et al.*<sup>11</sup> for Rene88DT. Therefore, one may conclude for the above argument that the cooling rate from solution or partial solution temperatures can affect the microstructure of superalloys after aging in different ways that depend on the composition of these alloys.

The superior tensile and stress rupture properties of IN792 relative to IN738LC made this alloy a good candidate for use in gas turbine blades.<sup>12</sup> However, to the best knowledge of the authors, there is no comprehensive published report on the effect of cooling rate on the microstructure of IN792 during cooling with various rates from partial solution temperature and the proceeding aging. Thus, the aim of the present research is to clarify these effects to some extent.

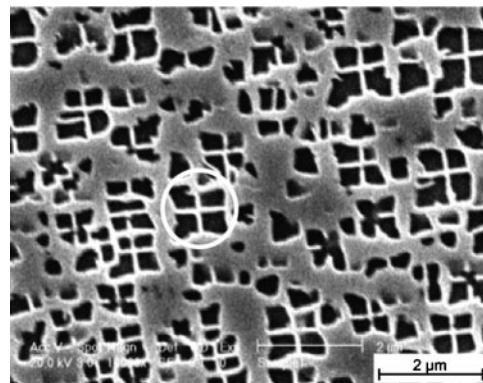
## Experimental

The mean chemical composition of the IN792 superalloy used in the present research is Ni-0.08C-3.4Al-0.14Fe-0.03Si-8.8Co-12.6Cr-1.8Mo-4Ti-4.23W-4.1Ta (wt-%). The initial bars of IN792 were cast in vacuum  $10^{-3}$  bar in an inductive furnace. These bars were solution treated at 1200°C for 2 h. Then they were subjected to partial solution treatment at 1120°C for 2 h, before cooling them to room temperature with controlled cooling rates of 5, 20, 30, 60, 90, 120 and 160°C min<sup>-1</sup>. Then, several samples were prepared from each partially treated bar before subjecting them to aging at 845°C for 24 h and cooling them to room temperature in air. The heat treatment cycles applied to the cast bars are shown schematically in Fig. 1.

After preparing samples in a routine metallographic way, the microstructures were examined by scanning electron microscopy (SEM). The etchant used in the present study was 25 mL lactic acid+15 mL HNO<sub>3</sub>+1 mL HF. Quantitative measurement of  $\gamma'$  precipitates was performed by an image analyser; however, the size distribution of the tiny particles was not established due to the lack of access to transition electron microscopy.

## Results

The typical as cast microstructure of IN792 superalloy is presented in Fig. 2. The microstructure of the as cast sample contained basically  $\gamma$  matrix and cubic primary  $\gamma'$  precipitates in a butterfly shape (e.g. *see* inside inserts in Fig. 2). The cast microstructure after being subjected to



2 Microstructure of IN792 cast alloy

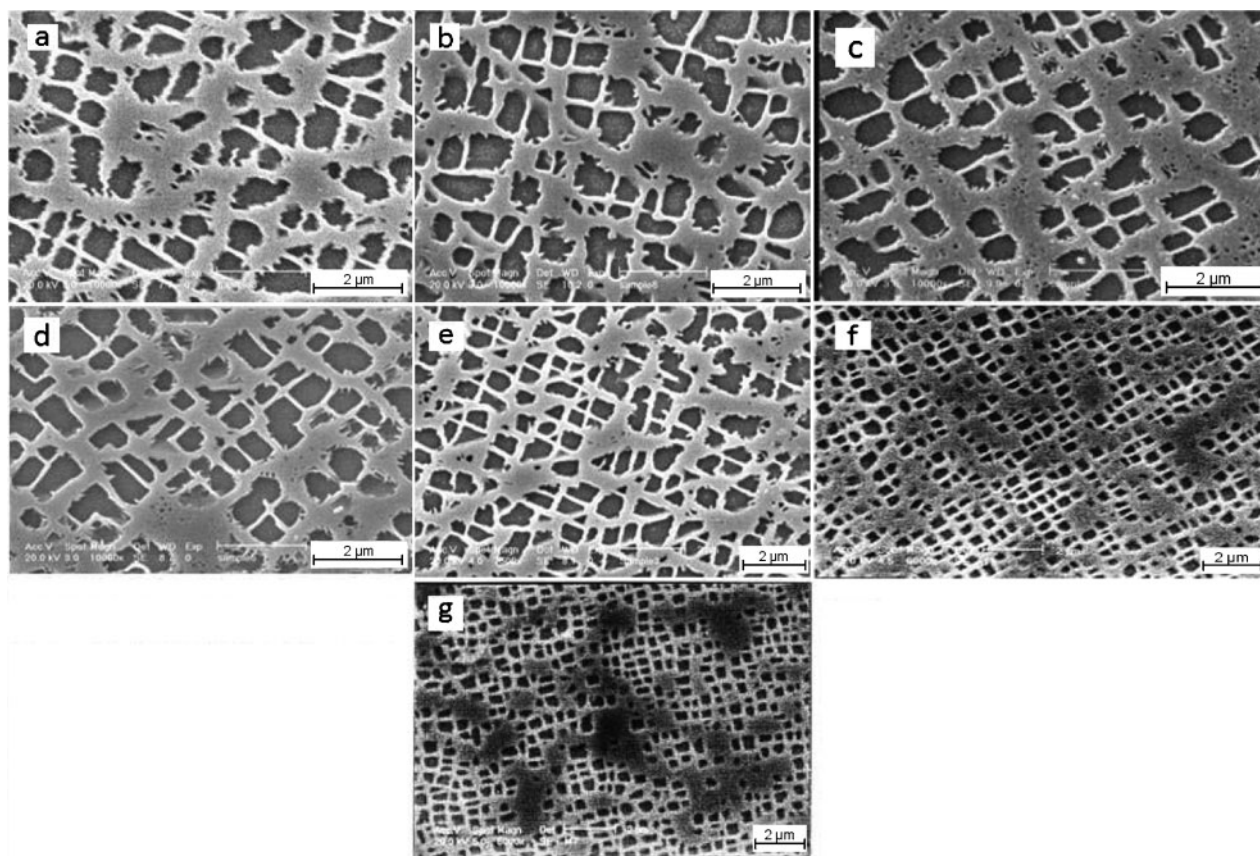
partial solution treatment and cooled with different cooling rates to room temperature changed enormously as shown in various micrographs in Fig. 3. These micrographs show at a very low cooling rate of 5°C min<sup>-1</sup> a few number of secondary  $\gamma'$  particles precipitated and grown together with primary  $\gamma'$  during cooling from partial solution temperature. By increasing the cooling rate from 10 to 60°C min<sup>-1</sup>, the number of small spherical secondary  $\gamma'$  precipitates increased, while at higher cooling rates up to 160°C min<sup>-1</sup> only few secondary  $\gamma'$  precipitated during cooling from partial solution temperature. In addition, at cooling rates higher than 60°C min<sup>-1</sup>, the shape of primary  $\gamma'$  was different to those observed earlier in samples cooled with lower rates. In other words, cubic  $\gamma'$  was the dominant shape observed.

The SEM microstructures of the samples after aging are shown in Fig. 4. This figure shows that the mean size of the  $\gamma'$  particles in all of the samples slightly increased relative to the samples in partial solution conditions. In addition, a large number of secondary  $\gamma'$  appeared in the matrix of the samples that had cooling rates >60°C min<sup>-1</sup>.

Figures 5 and 6 show by increasing the cooling rate that the mean size of the primary  $\gamma'$  particles decreased, while during subsequent aging it increased substantially. Increasing the cooling rate from 5 to 160°C min<sup>-1</sup> caused the mean size of the primary  $\gamma'$  particles to reduce from 680 to 510 nm, but during aging more growth was observed on the samples that had higher cooling rate from partial solution temperature. For example, the mean size of primary  $\gamma'$  particles after aging for cooling rate of 5°C min<sup>-1</sup> was 730 nm, which means 7% increase in their mean size, while the mean size of these particles after aging for cooling rate of 160°C min<sup>-1</sup> was 620 nm, which means 17% increase in their mean size.

Similarly, the mean size of the secondary  $\gamma'$  particles after aging decreased with increasing aging temperature but with a decelerating rate, as shown in Fig. 6. For example, the sizes of secondary  $\gamma'$  particles after aging for cooling rates of 5 and 160°C min<sup>-1</sup> were 180 and 96 nm respectively.

Changes in volume fraction of secondary  $\gamma'$  particles after aging are shown in Fig. 7. This figure shows that increasing the cooling rate from partial solution temperature severely affected the precipitation behaviour of  $\gamma'$  particles after aging. The higher the cooling rate, the higher the volume fraction of secondary  $\gamma'$



3 Microstructures of IN792 after partial solution treatment at 1120°C for 2 h and different cooling rates of a 5°C min<sup>-1</sup>, b 20°C min<sup>-1</sup>, c 30°C min<sup>-1</sup>, d 60°C min<sup>-1</sup>, e 90°C min<sup>-1</sup>, f 120°C min<sup>-1</sup> and g 160°C min<sup>-1</sup>

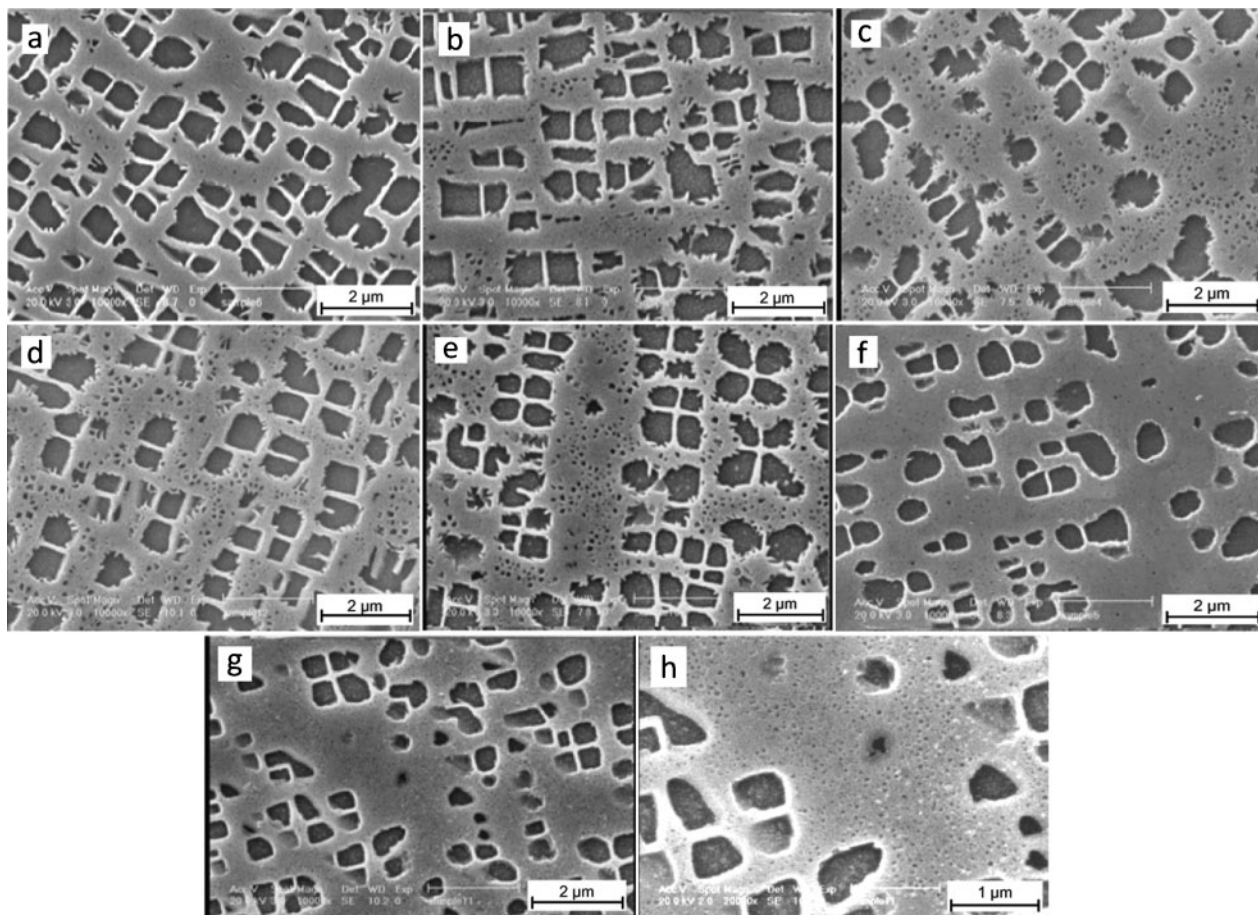
particles after aging. However, the increasing rate of volume fraction of secondary  $\gamma'$  particles after aging reduces with increasing cooling rate, so that the use of cooling rates  $>60^\circ\text{C min}^{-1}$  caused the volume fraction of secondary  $\gamma'$  particles to increase linearly with a very small slope rather than exponentially, as shown by the broken line in Fig. 7.

## Discussion

The formation of secondary  $\gamma'$  phase within the matrix requires, first of all, some parts of the matrix to become rich in specific elements, and then these rich areas transform to new phase out of the host matrix, as the classical nucleation theory states.<sup>13</sup> The critical radius for nucleation depends basically on two factors: 1) free chemical energy of the super saturated matrix and 2) interface energy of  $\gamma$  and  $\gamma'$  particles. Increasing the cooling rate from solution temperature causes the degree of supersaturation to increase, as has been reported by Mao *et al.*,<sup>11</sup> and the coherent strain energy between  $\gamma$  and  $\gamma'$  to decrease according to Mitchell *et al.*<sup>14</sup> Both of the abovementioned phenomena can cause a reduction in the radius of the critical nuclei, so the nucleation of  $\gamma'$  precipitates from the  $\gamma$  matrix with smaller critical radius becomes possible. Therefore, when the rate of cooling from solution temperature was low (i.e.  $5\text{--}20^\circ\text{C min}^{-1}$ ), the energy barrier for nucleation was high, so that the elements required for the formation of new  $\gamma'$  particles diffuse preferably into the existed primary  $\gamma'$  particles and caused their growth rather than be used for the formation of new  $\gamma'$  particles (*see* Figs. 2 and 5). Thus, as it can be seen in the microstructures presented in

Fig. 3 and the graph in Fig. 7, very limited number of secondary  $\gamma'$  particles were formed during cooling from solution temperature.

When the cooling rate increases up to  $60^\circ\text{C min}^{-1}$ , higher nucleation of secondary  $\gamma'$  particles occurs during cooling, as Figs. 3 and 7 indicate; however, further increase in the cooling rate severely reduced the diffusion time required for the elements, so no newly secondary  $\gamma'$  particles can be precipitated during cooling from partial solution temperature. Under these conditions, a very limited amount of growth in the primary  $\gamma'$  particles during cooling was possible. Therefore, when a very high cooling rate of  $>90^\circ\text{C min}^{-1}$  from the solution temperature was used, an ignorable number of secondary  $\gamma'$  particles were detected within the microstructure of the matrix (*see* Fig. 3e–g). This seems to relate to the very limited time available for diffusion of elements required for the formation of  $\gamma'$  particles within the matrix. Therefore, due to the low diffusion rate, the required critical Gibbs free energy for nucleation was so high in value that neither formation of new secondary  $\gamma'$  particles nor the growth of existing primary  $\gamma'$  particles during cooling was noticeable. Instead, for high cooling rates of 120 and  $160^\circ\text{C min}^{-1}$ , highly contrasted zones due to segregation of some elements [which can distort the surrounding lattice (without changing the matrix structure), causing local variation in the intensity of electron diffraction (similar to the image of Guinier–Preston zones in Al–Cu alloys, or with some reservations the images produced during diffusionless transformation of austenite to martensite, *see* section 6 in Ref. 15), which in turn shows up as a variation in image intensity] can be observed (*see* Fig. 3f and g). These zones can

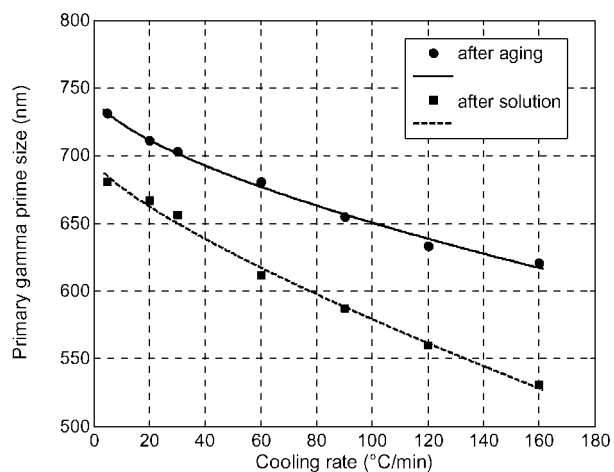


a 5°C min<sup>-1</sup>; b 20°C min<sup>-1</sup>; c 30°C min<sup>-1</sup>; d 60°C min<sup>-1</sup>; e 90°C min<sup>-1</sup>; f 120°C min<sup>-1</sup>; g and h 160°C min<sup>-1</sup>  
**4 Microstructures of IN792 after aging samples cooled at different rates at 845°C for 24 h**

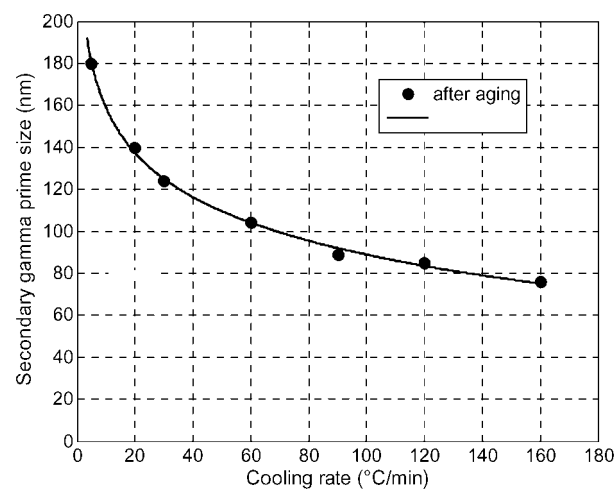
provide the required conditions for precipitation of secondary  $\gamma'$  particles during the subsequent aging.<sup>15</sup> Since after aging there is a driving force for precipitation of the equilibrium  $\gamma'$  phase, secondary  $\gamma'$  particles precipitate, causing a substantial reduction in the matrix lattice distortion, so that the zone contrast observed after cooling disappeared after aging.

As indicated above, high cooling rates, particularly the cooling rates of 120 and 160°C min<sup>-1</sup>, caused suppression of elemental diffusion within the matrix; hence, the formation of secondary  $\gamma'$  particles during

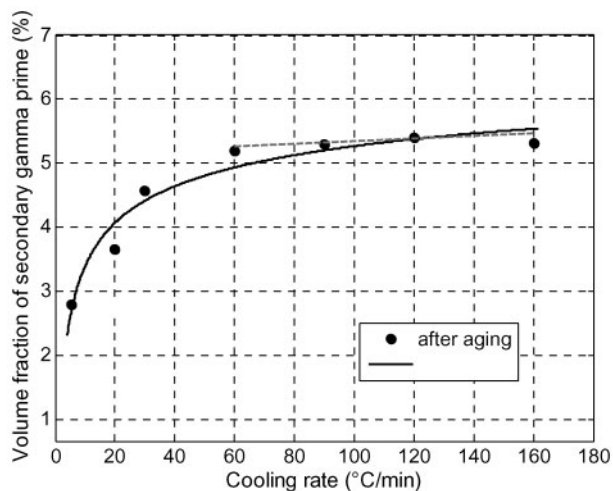
cooling was suspended. In other words, enough elements required for precipitation during aging remained within the supersaturated matrix. On the other hand, since the substrate contains a large number of heterogeneously dispersed in-grown dislocations as well as a great deal of solute atoms, one expects that the nucleation of secondary  $\gamma'$  particles occurs heterogeneously as the kinetic of precipitation of particles varies with dislocation densities within the matrix. The size and numbers of nuclei depended on the degree of supersaturation and



**5 Variation of primary gamma prime size with different cooling rates from partial solution temperature**



**6 Variation of secondary gamma prime size with different cooling rates from partial solution temperature**



7 Variation of volume fraction of secondary gamma prime size after aging with different cooling rates from partial solution temperature

the number of stress concentration points (e.g. dislocation density in this case) exiting in the matrix. Where the saturation degree and the stress concentration points were high, the number of secondary  $\gamma'$  particles formed during aging was also very high (see Fig. 4). This argument is visualised in Fig. 7. These figures show at cooling rates  $>60^{\circ}\text{C min}^{-1}$  that the combination of higher degree of elemental saturation zones and high number of stress concentration zones caused the formation of a large amount of very small secondary  $\gamma'$  particles within the supersaturated matrix during aging.

Another phenomenon observed in the microstructure of this alloy under all conditions, i.e. cast, solution treated and aged, was that the primary  $\gamma'$  particles appeared with a butterfly shape morphology. The observation of this type of  $\gamma'$  outlook is said<sup>16</sup> to be due to the partitioning phenomenon that occurs during heat treatment, but in the current research this configuration of primary  $\gamma'$  was also observed in the cast alloy (Fig. 2). This observation confirms the idea that the partitioning phenomenon that occurs during heat treatment is not necessary the only partitioning mechanism for creating such morphology for primary  $\gamma'$ . The particles formed during casting had no enough time for growth and partitioning; therefore, other mechanisms may have been operative for the formation of this type of morphology. A few years ago Zhang *et al.*<sup>17</sup> reported that elements such as Ti, Ta and Cr severely segregate within the last portion of the melt during solidification of IN792. Considering this argument, it seems the segregation of the element, such as Al, Ti, Ta and Cr, which is required for the formation of primary  $\gamma'$  particles during solidification, caused the formation of

very rich zones from those elements during this process. Therefore, during cooling of the melt, the chance of nucleation of more than one nucleus in any segregated zone was more; thus, several primary  $\gamma'$  particles nucleated close to each other and grew as far as the required species for growth were available within the segregated matrix. The above argument requires further investigation.

## Conclusions

1. The microstructural features of IN792 are sensitive to the cooling rate from partial solution, so that by increasing this cooling rate from  $5$  to  $160^{\circ}\text{C min}^{-1}$  the amounts of small secondary  $\gamma'$  particles increase with a decelerating rate during aging of this alloy.

2. By increasing the cooling rate, the sizes of primary and secondary  $\gamma'$  particles decrease in the microstructure of superalloy IN792.

## Acknowledgements

The authors like to thank engineers M. Cheraghzadeh and Y. Milladi from Mavadkaran Eng. Co for supporting this project.

## References

1. N. Das: *Trans. Indian Inst. Met.*, 2010, **63**, 265–274.
2. M. J. Donachie and S. J. Donachie: 'Superalloys: a technical guide'; 2002, Materials Park, OH, ASM International.
3. M. Jackson and R. Reed: *Mater. Sci. Eng. A*, 1999, **A259**, 85–97.
4. R. Sharghi-Moshtaghin and S. Asgari: *J. Mater. Process. Technol.*, 2004, **147**, 343–350.
5. S. A. Sajjadi, S. M. Zebarjad, R. Guthrie and M. Isac: *J. Mater. Process. Technol.*, 2006, **175**, 376–381.
6. H. Monajati, M. Jahazi, R. Bahrami and S. Yue: *Mater. Sci. Eng. A*, 2004, **A373**, 286–293.
7. A. K. Koul, R. Castillo, V. P. Swaminathan and N. S. Cheruvu: 'Advanced materials and coatings for combustion turbines', Proc. ASM 1993 Materials Cong. Materials Week, ASM International, Pittsburg, PA, USA, October 1993, 17–21.
8. F. Torster, G. Baumeister, J. Albrecht, G. Lütjering, D. Helm and M. Daeubler: *Mater. Sci. Eng. A*, 1997, **A234**, 189–192.
9. F. Blum, J. Benson and C. Stander: *J. Mater. Sci. Lett.*, 1994, **13**, 1213–1214.
10. S.A. Sajjadi, H. Elahifar and H. Farhangi: *J. Alloys Compd*, 2008, **455**, 215–220.
11. J. Mao, K. M. Chang, W. Yang, D. U. Furrer, K. Ray and S. P. Vaze: *Mater. Sci. Eng. A*, 2002, **A332**, 318–329.
12. G. L. Erickson: 'Metals handbook', 10th edn, Vol. 1, 981–994; 1990, Materials Park, OH, ASM international.
13. R. Reed-Hill and R. Abbaschian: 'Physical metallurgy principles'; 1994, Boston, MA, PWS Publishing Company.
14. R. Mitchell, M. Preuss, M. Hardy and S. Tin: *Mater. Sci. Eng. A*, 2006, **A423**, 282–291.
15. D. A. Porter and K. E. Easterling: 'Phase transformations in metals and alloys', Vol. 5, 290–300; 1983, Berkshire, Van Nostrand Reinhold Co. Ltd.
16. M. Doi, T. Miyazaki and T. Wakatsuki: *Mater. Sci. Eng.*, 1984, **67**, 247–253.
17. J. Zhang and R. Singer: *Acta Mater.*, 2002, **50**, 1869–1879.